Dual AAV Gene Therapy for Duchenne Muscular Dystrophy with a 7-kb *Mini-Dystrophin* Gene in the Canine Model

Kasun Kodippili,[1] Chady H. Hakim,[1,2] Xiufang Pan,[1] Hsiao T. Yang,[1,3] Yongping Yue,[1] Yadong Zhang,[1,†] Jin-Hong Shin,[1,‡] N. Nora Yang,[2] and Dongsheng Duan,[1,3,4,5,*]

Departments of [1]Molecular Microbiology and Immunology and [4]Neurology, School of Medicine, [3]Department of Biomedical Sciences, College of Veterinary Medicine, and [5]Department of Bioengineering, The University of Missouri, Columbia, Missouri; [2]National Center for Advancing Translational Sciences, Bethesda, Maryland.
†Current affiliation: The Central Hospital of Wuhan, Huazhong University of Science and Technology, Wuhan, Hubei, China.
‡Current affiliation: Department of Neurology, Pusan National University Yangsan Hospital, Yangsan, Republic of Korea.

Dual adeno-associated virus (AAV) technology was developed in 2000 to double the packaging capacity of the AAV vector. The proof of principle has been demonstrated in various mouse models. Yet, pivotal evidence is lacking in large animal models of human diseases. Here we report expression of a 7-kb canine *Δ*H2–R15 *mini-dystrophin* gene using a pair of dual AAV vectors in the canine model of Duchenne muscular dystrophy (DMD). The *Δ*H2–R15 minigene is by far the most potent synthetic *dystrophin* gene engineered for DMD gene therapy. We packaged minigene dual vectors in Y731F tyrosine-modified AAV-9 and delivered to the extensor carpi ulnaris muscle of a 12-month-old affected dog at the dose of 2×10^{13} viral genome particles/vector/muscle. Widespread mini-dystrophin expression was observed 2 months after gene transfer. The missing dystrophin-associated glycoprotein complex was restored. Treatment also reduced muscle degeneration and fibrosis and improved myofiber size distribution. Importantly, dual AAV therapy greatly protected the muscle from eccentric contraction-induced force loss. Our data provide the first clear evidence that dual AAV therapy can be translated to a diseased large mammal. Further development of dual AAV technology may lead to effective therapies for DMD and many other diseases in human patients.

Keywords: dystrophin, Duchenne muscular dystrophy, canine model, adeno-associated virus, dual AAV vectors, mini-dystrophin

INTRODUCTION

DYSTROPHIN GENE MUTATION leads to Duchenne muscular dystrophy (DMD), a severe disease that results in body-wide muscle degeneration and necrosis in boys and young men. Adeno-associated virus (AAV)–mediated *dystrophin* gene replacement therapy is being actively pursued to treat DMD. The 12-kb full-length *dystrophin* gene cDNA was cloned in 1987.[1,2] The 427-kD full-length protein is a subsarcolemmal cytoskeletal protein and has four major domains including the N-terminal, rod, cysteine-rich (CR), and C-terminal (CT) domains. The rod domain can be further divided into 24 spectrin-like repeats (R) and four proline-rich hinges (H). Dystrophin assembles a number of cytosolic and transmembrane proteins into the dystrophin-associated glycoprotein complex (DGC) to protect the sarcolemma from mechanical stress generated during muscle contraction.

The AAV vector is the leading vector for muscle gene therapy. However, its maximal packaging capacity is only 5 kb.[3–5] This is clearly not enough for the 12-kb full-length dystrophin cDNA. To overcome this hurdle, investigators have synthesized super-small microgenes. Micro-dystrophins are about one-third the size of the full-length protein. Although micro-dystrophin can protect dystrophic mice, it is unclear how it will fare in human muscle. In this regard, it is worth to point out that a patient who expressed a truncated in-frame dystrophin protein of a similar size to that of micro-dystrophin was shown to display severe disease.[6]

*Correspondence: Dr. Dongsheng Duan, Department of Molecular Microbiology and Immunology, M610 Medical Sciences Building, One Hospital Drive, Columbia, MO 65212. E-mail: duand@missouri.edu

DOI: 10.1089/hum.2017.095

In 1990, the Davies lab discovered a half-size *dystrophin* gene from a patient who was ambulant at age 61 years.[7] The cDNA of this truncated gene is termed the *mini-dystrophin* gene. The minigene is 6.2-kb and contains an incomplete repeat 19 (R19).[7] The partial repeat disrupts the normal phasing of the protein. In 2002, the Chamberlain lab engineered the 6-kb *Δ*H2–R19 minigene.[8] The residual R19 was removed in this minigene. The 6-kb minigene yielded much better functional rescue than the original 6.2-kb minigene in transgenic mice.[8] Unfortunately, none of these minigenes carry the pivotal R16/17 neuronal nitric oxide synthase (nNOS)-binding domain.[9,10] To address this issue, we developed a 6-kb *Δ*R2–15/*Δ*R18–19 minigene by replacing R2 and R3 in the Chamberlain version minigene with R16 and R17.[11] Preliminary studies in mouse models of DMD show that this new 6-kb minigene normalized nNOS homeostasis, reduced muscle pathology and improved muscle contractility.[12] We recently discovered that R1-3 represents a previously unappreciated membrane-binding domain in dystrophin.[13] In light of this new finding, we decided to shift our emphasis to the R1-3 containing 7-kb *Δ*H2–R15 *mini-dystrophin* gene.[9]

In order to deliver the minigene with AAV, we have previously invented the dual AAV technology.[14–18] In this technology, an intact expression cassette is split into two parts and each part is delivered by an AAV vector. Co-infection of both vectors reconstitutes transgene expression (reviewed elsewhere[19–21]). In a series of studies, we and others have further demonstrated that local and systemic delivery of the 6-kb minigene with dual AAV can lead to highly efficient mini-dystrophin expression and muscle protection in dystrophic mice.[11,12,17,22–25] Here we tested the hypothesis that dual AAV gene therapy can effectively reconstitute the 7-kb *Δ*H2–R15 minigene expression in the canine DMD model. We found encouraging proof of principle evidence that dual AAV-mediated gene therapy with the 7-kb *Δ*H2–R15 minigene can greatly reduce muscle pathology and improve muscle function in an adult dystrophic dog.

MATERIALS AND METHODS

Animals

All animal experiments were approved by the Animal Care and Use Committee of the University of Missouri and were performed in accordance with U.S. National Institutes of Health guidelines. A 12-month-old affected dog (ID# dog E25) was selected to receive dual AAV local injection based on the availability of the dogs in the colony at the time of the study. This dog had a mixed genetic background of golden retriever, labrador retriever, and beagle. It carried a point mutation in intron 6 that disrupted dystrophin RNA splicing and the resulting transcript contained a frame-shift mutation and a premature stop codon. In addition, 11 adult normal dogs (age: 14.53 ± 5.77 months) and 12 adult dystrophic dogs (age: 8.78 ± 3.76 months) were used as controls. All experimental dogs were on a mixed genetic background and generated in house by artificial insemination. All affected dogs carry mutations in the *dystrophin* gene that abort dystrophin expression. The genotype was determined by polymerase chain reaction according to published protocols.[26–28] The diagnosis was also confirmed by the significantly elevated serum creatine kinase level in affected dogs.

All experimental dogs were housed in a specific-pathogen-free animal care facility and kept under a 12-h light/12-h dark cycle. Affected dogs were housed in a raised platform kennel, while normal dogs were housed in a regular floor kennel. Depending on the age and size, two or more dogs are housed together to promote socialization. Normal dogs were fed dry Purina Lab Diet 5006, while affected dogs were fed wet Purina Proplan Puppy food. Dogs were given *ad libitum* access to clean drinking water. Toys were allowed in the kennel with dogs for enrichment. Dogs were monitored daily by the caregiver for overall health condition and activity. A full physical examination was performed by the veterinarian from the Office of Animal Research at the University of Missouri for any unusual changes (such as behavior, activity, food and water consumption, and clinical symptoms). The body weight of the dogs was measured periodically to monitor growth. Experimental subjects were euthanized at the end of the study according to the 2013 American Veterinary Medical Association Guidelines for the Euthanasia of Animals.

Mini-dystrophin dual AAV vector construction and recombinant Y731F tyrosine mutant AAV-9 production

The proviral *cis* plasmids used in this study included YZ37 and YZ39 (Fig. 1). They were generated by standard molecular cloning techniques. YZ37 contains the cytomegalovirus (CMV) promoter, a flag tag fused to the N-terminal end of the *dystrophin* gene, and the 5′ half of the *Δ*H2–R15 *mini-dystrophin* gene (including the N-terminal domain, hinges 1 and 3, and spectrin-like repeats R1, R2, R3, R16, R17, R18, R19, R20 and part of R21). YZ39 contains the 3′ half of the *Δ*H2–R15 *mini-dystrophin* gene (including a part of hinge 3, spectrin-like

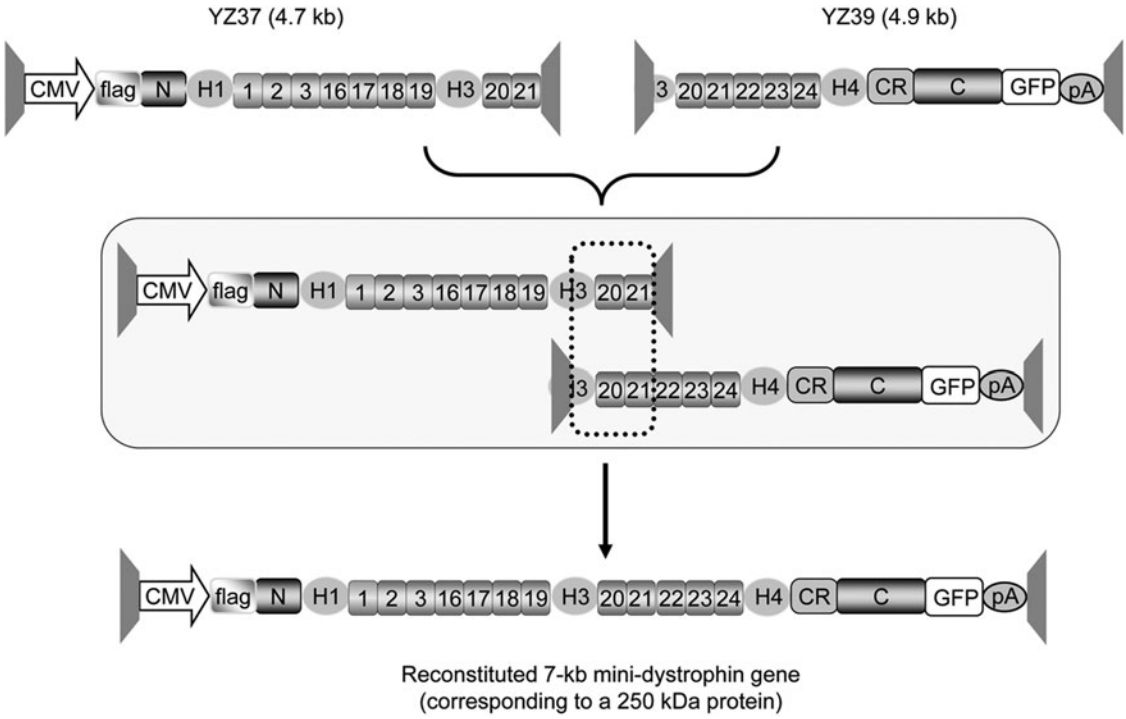

Figure 1. A schematic outline of the dual AAV ΔH2–R15 mini-dystrophin vectors. YZ37 (vector size = 4.7 kb) carries the 5′ part of the minigene and YZ39 (vector size = 4.9 kb) carries the 3′ part. A flag gene is fused in-frame to the N-terminal end of the *mini-dystrophin* gene and a GFP gene is fused in-frame to the C-terminal end. Homologous recombination between the overlapping region (indicated by *dotted box*) reconstitutes the complete 7-kb *mini-dystrophin* gene expression cassette (size = 8.6 kb) and leads to the production of a 250-kD mini-dystrophin protein). AAV, adeno-associated virus; C, C-terminal domain of dystrophin; CMV, cytomegalovirus promoter; CR, cysteine-rich domain of dystrophin; H, proline-rich hinges in the dystrophin rod domain; N, N-terminal domain of dystrophin; pA, polyadenylation signal; trapezoid structures, inverted terminal repeats of AAV. Numerical digits, spectrin-like repeats (R) in the dystrophin rod domain.

repeats R20 to R24, hinge 4, the cysteine-rich domain and the C-terminal domain), a green fluorescent protein (GFP) tag fused to the C-terminal end and the SV40 polyadenylation signal. A 0.4-kb *dystrophin* gene fragment (from the late part of hinge 3 to the first part of R21) was shared by YZ37 and YZ39 vectors (Supplementary Fig. S1; Supplementary Data are available online at www.liebertpub.com/hum).

The Y731F AAV-9 capsid-packaging construct was a generous gift from Dr. Arun Srivastava (University of Florida, Gainesville, FL).[29] Recombinant vector stock was generated using the transient transfection protocol and purified through three rounds of cesium chloride ultracentrifugation according to our published protocols.[30] We have previously demonstrated that Y731F AAV-9 can lead to efficient local and systemic gene transfer in dystrophic dog muscle.[31–33] Viral titer was determined using the Fast SYBR Green Master Mix kit (Bio-Rad, Hercules, CA) by real-time quantitative PCR (qPCR) in an ABI 7900 HT qPCR machine (Applied Biosystems, Foster City, CA).

Immune suppression and gene delivery

Immunosuppression was applied starting from 1 week before AAV injection and continued through the course of the study (8 weeks). Cyclosporine (Neoral, 100 mg/mL; Novartis, East Hanover, NJ; NDC 0078-0274-22) and mycophenolate mofetil (CellCept, 200 mg/mL; Genentech, South San Francisco, CA; NDC 0004-0261-29) were used to achieve immunosuppression.[31,34] Cyclosporine was administered orally at the dose of 10–20 mg/kg·day to achieve a whole blood trough level of 100–200 ng/mL. The cyclosporine level was measured at the Clinical Pathology Laboratory in the University of Missouri Hospital (Columbia, MO). The blood trough level was achieved at day 6 day after starting cyclosporine. Mycophenolate mofetil was administered orally twice a day at the dose of 20 mg/kg (40 mg/kg·day).

The dog was awake throughout the injection. Briefly, the dog was gently restrained on the surgery table and the extensor carpi ulnaris (ECU) muscle was identified according to anatomical markings as we have previously described.[31] A total of 2×10^{13} vector genome (vg) particles/vector were

delivered to the right ECU muscle in five separate injections (0.4 mL per injection) in a total volume of 2 mL. An equal volume of HEPES (N-2-hydroxyethylpiperazine-N-2-ethane sulfonic acid) buffer was injected into the left ECU. The dog was injected at 12 months of age and AAV transduction was evaluated 2 months later.

AAV genome copy number quantification

Freshly dissected muscles were snap-frozen in liquid nitrogen–cooled isopentane in the optimal cutting temperature compound (OCT) (Sakura Finetek Inc., Torrance, CA). Genomic DNA was extracted from OCT-embedded tissue samples. DNA concentration was quantified with Qubit dsDNA HS assay kit (ThermoFisher Scientific, Waltham, MA). TaqMan assays were designed to detect the vector genome copy number for YL37 and YL39. Specifically, we designed an assay to detect R3-R16 junction in YL37. We also designed as assay to detect the SV40 polyadenylation signal in YL39. For R3–16 detection, the forward primer is 5′ AGTCA AGCGCCCAGATCAG, the reverse primer is 5′ AGA CATGGGTGATCTCAGTCAGA, and the probe is 5′ CCAGGCTGTGGAAATT. For SV40 pA detection, the forward primer is 5′ ACAAACCACAACTAGAA TGCAGTGA, the reverse primer is 5′ TGTTGTTGT TAACTTGTTTATTGCAGCTTA and the probe is 5′ ATAGCATCACAAATTTC. Quantitative TaqMan PCR assays were performed using the TaqMan Universal PCR master mix (ThermoFisher Scientific). The threshold cycle value of each reaction was converted to the vector genome copy number by measuring against the copy number standard curve of the known amount of the respective proviral *cis* plasmid (YL37 or YL39). The data are reported as the vg copy number per diploid genome.

Histopathology

Hematoxylin and eosin (HE) staining was used to study the general histopathology. Fibrosis was evaluated by Masson trichrome staining using a kit from Richard-Allan Scientific (Kalamazoo, MI). Dystrophin expression was detected using seven dystrophin-specific antibodies according to our published protocols.[36] The N-terminal domain of dystrophin was detected with a rabbit polyclonal antibody (1:600) (a gift from Dr. Jeffrey Chamberlain at the University of Washington). Spectrin-like repeats 4–6 (R4–6) was detected with the H-300 rabbit polyclonal antibody (1:400; Santa Cruz Biotechnology, Santa Cruz, CA). R11 was detected with Mandys8 (1:200; Sigma, St Louis, MO). R16 was detected with Mandys103 (1:20; a gift from Dr. Glenn Morris at the Robert Jones and Agnes Hunt Orthopaedic Hospital (Oswestry, UK). R17 was detected with Manex 44A (1:500; a gift from Dr. Glenn Morris). H3 was detected with Manex 50 (1:2,000; a gift from Dr. Glenn Morris). The C-terminal domain was detected with Dys2 (1:20; Novocastra, Newcastle, UK). The dystrophin-associated glycoprotein complex (DGC) components were evaluated with monoclonal antibodies against β-dystroglycan (1:50; Novocastra, Newcastle, UK), β-sarcoglycan (1:50; Novocastra), dystrobrevin (1:200; BD Bioscience, San Diego, CA), and syntrophin (1:200; Abcam, Cambridge, MA).

Slides were viewed using a Nikon E800 fluorescence microscope. Photomicrographs were taken with a QImage Retiga 1300 camera. Central nucleation and the myofiber diameter were determined from five or more random microscopic fields of an HE-stained muscle section. The myofiber size was determined from the digitized images using the quantitative image analysis module of the extended version of the Photoshop CS5.5 software as we published before (Photoshop version CS5.5 extended; Adobe Systems Incorporated, San Jose, CA).[31,35]

Western blot

Whole muscle lysate was prepared from liquid nitrogen preserved ECU muscle tissue as described previously.[36] Muscle lysates were resolved on a 6% sodium dodecyl sulfate-polyacrylamide gel and protein was transferred to a polyvinylidene difluoride membrane. Dystrophin was detected with a monoclonal antibody against the C-terminal domain (Dys2, 1:100 dilution, clone Dy8/6C5, IgG1; Novocastra, Newcastle, UK). This antibody recognized both full-length dystrophin and ΔH2–R15 mini-dystrophin.

Muscle function assay

The ECU muscle force was evaluated using our previously published protocol.[31,35] The dog was sedated with ketamine (15 mg/kg body weight) and acepromazine (0.12 mg/kg bdy weight). Anesthesia was induced with 4% isoflurane and maintained with 2% isoflurane. The dog was placed in the supine position on a custom-made *in situ* muscle function assay setup. A catheter was placed in the thoracic aorta to monitor blood pressure. Another catheter was placed in the jugular vein for lactated saline infusion. Core body temperature was monitored and maintained at 37°C throughout the assay. The entire ECU muscle was surgically exposed and the distal tendon was attached to the force transducer (SM-250-38; Interface, Scottsdale, AZ) at the distal tendon. The radial nerve was carefully

dissected and mounted on a bipolar electrode using 8 volts and 0.2-ms pulse duration electric stimulation (Grass S48 Stimulator, Grass Instruments, Quincy, MA). The optimal muscle length (L_o) was determined using single twitch stimulation. The tetanic force was determined by applying 200-ms tetanic stimulation at the frequency of 100 Hz. The physiological cross-sectional area (PCSA) was calculated according to the equation PCSA = (muscle weight in grams $\times \cos[10.03]$)/(1.06 g/cm^3 $\times$ optimal fiber length in cm), where 1.06 g/cm^3 is the muscle density and 10.03 is the pennation angle of the ECU muscle.[35] The optimal fiber length (L_f) was determined by multiplying the measured L_o of the muscle by the ECU muscle L_f/L_o ratio of 0.0448.[35] The specific muscle force was calculated by normalizing the absolute tetanic muscle force by the PCSA. Following a 20-min rest, the muscle was subjected to 10 cycles of eccentric contraction. In each cycle, the muscle was stimulated to reach the maximal tetanic force for a total time of 1,200 ms. In the last 1,100 ms the ECU muscle was stretched by $\sim$5% of its original length. After a 2-min rest, a second cycle of eccentric contraction was applied. The percentage of force drop after each cycle of eccentric contraction was calculated. The dog was euthanized at the end of the assay and tissues collected for further analysis.

RESULTS

Construction of the ΔH2–R15 mini-dystrophin dual AAV vectors

We have previously shown that the *Δ*H2–R15 minigene can restore skeletal muscle and heart function in transgenic mdx mice.[9,37] This minigene encodes a 250-kD protein. Specifically, it contains the actin-binding domain, R1–3 membrane binding domain, R16/17 nNOS-binding domain, R16–19 putative heart protection domain, R20–23 microtubule binding domain, dystroglycan binding domain, plectin binding domain, syntrophin and dystrobrevin binding domain, ankyrin binding domain, myospryn binding domain, and domains that interact with intermediate filaments such as synemin, synemin-2, and keratin 19 (Duan lab, unpublished data).[9,10,13,38–51] In the middle of the dystrophin cDNA, there is a 0.4-kb highly recombinogenic region (including part of hinge 3, whole R20, and part of R21) (Supplementary Fig. S1). This region has been used to generate dual and tri-AAV vectors to express the 6-kb *mini-dystrophin* gene and the full-length dystrophin cDNA.[11,25,52] Here, we also used this region to mediate reconstitution of the 7-kb *mini-dystrophin* gene (Fig. 1). Briefly, one vector (YZ37) carries the 5′-section of the minigene (from the N-terminal domain to R21) and the other vector (YZ39) carries the 3′-section of the minigene (from the second half of H3 to the C-terminal domain). As an additional means to validate the minigene reconstitution, we also engineered a flag tag at the N-terminal end and fused a *GFP* gene in frame at the C-terminal end (Fig. 1). The size of the completely reconstituted expression cassette is 8.6 kb (Fig. 1). It should also be mentioned that we built the 7-kb *mini-dystrophin* gene dual vector using the canine *dystrophin* gene because human dystrophin elicits strong cellular immune responses in dystrophic dogs.[34,53]

Dual AAV vectors expressed ΔH2–R15 mini-dystrophin in dystrophic dog muscle

To test whether dual AAV delivery can work in large mammals, we packaged the dual AAV *Δ*H2–R15 mini-dystrophin vectors in Y731F AAV-9 and co-delivered to the ECU muscle of a 12-month-old affected dog (dog E25) at the dose of 2×10^{13} vg particles/vector/muscle. The contralateral ECU muscle received the same volume HEPES buffer (excipient). To minimize vector-induced immune rejection, we applied immunosuppression using cyclosporine and mycophenolate mofetil. Two months following gene transfer, the subject was euthanized and we evaluated the AAV vector genome copy number, mini-dystrophin expression, DGC reconstitution, muscle histology and muscle force (Fig. 2A).

On flag antibody immunostaining, we detected widespread mini-dystrophin expression in the entire ECU muscle (Fig. 2B, Supplementary Fig. S2). On western blot, the molecular size of the reconstituted mini-dystrophin protein is identical to that of the intact mini-dystrophin protein expressed in transgenic mdx mice (Fig. 2C). Mapping with epitope-specific antibodies confirmed the composition of the reconstituted mini-dystrophin protein (Fig. 2D). Epitopes that are present in *Δ*H2–R15 mini-dystrophin showed positive staining (such as the N-terminus, R16, R17, H3, and C-terminus). Antibodies that are specific for the regions absent in *Δ*H2–R15 mini-dystrophin were negative in immunostaining (such as R4–6 and R11). Importantly, all dystrophin positive cells were also GFP positive, suggesting they are indeed reconstituted from dual AAV vectors rather than revertant myofibers (Fig. 2D).

On AAV genome quantification, we detected $\sim$200 to 250 vg copies per diploid genome of the two vectors (YL37 and YL39) in the injected ECU muscle (Fig. 3). Negligible vector genome copies were detected in distant muscles (such as the

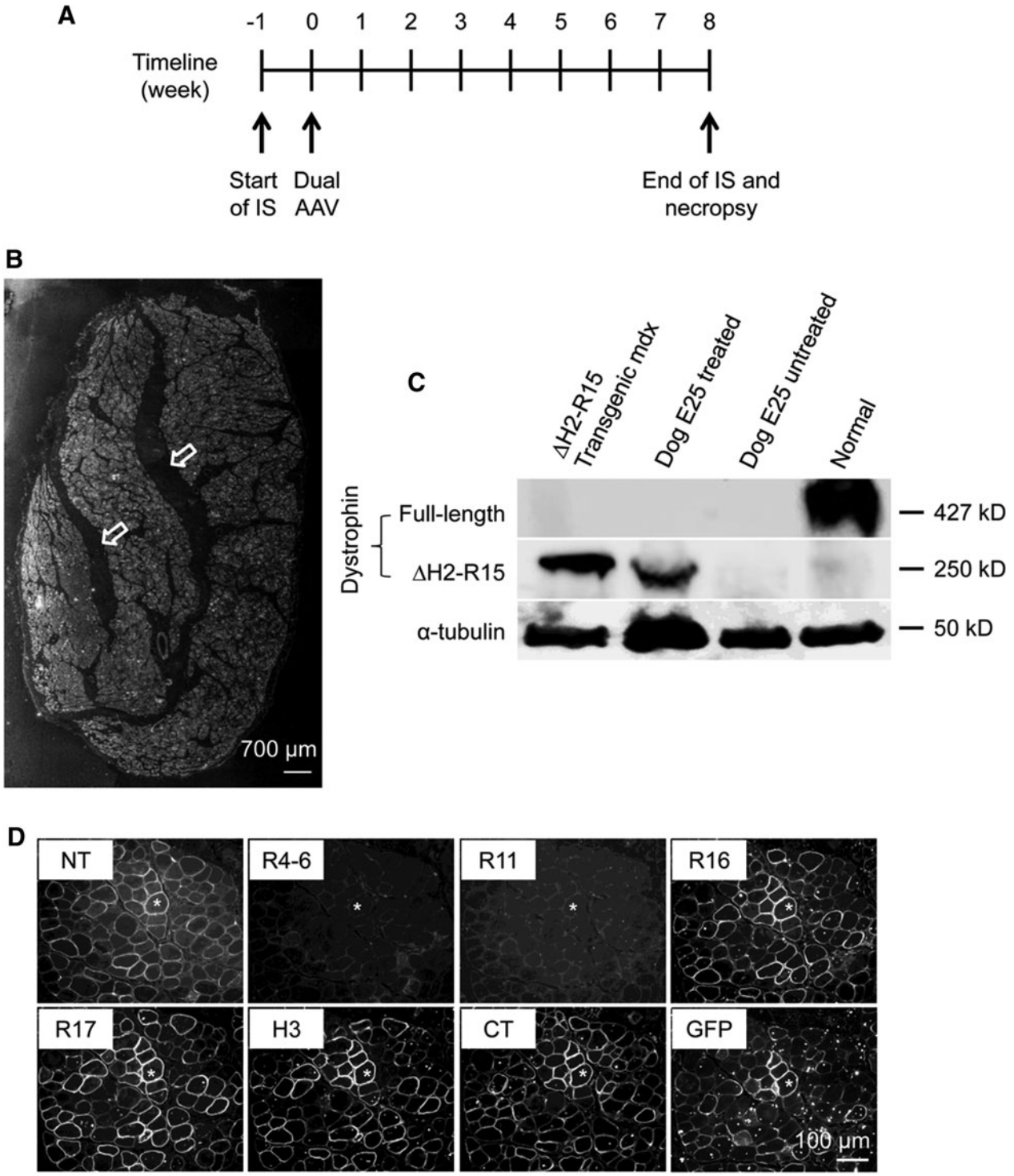

Figure 2. Intramuscular co-injection of minigene dual AAV vectors resulted in widespread mini-dystrophin expression **(A)** Schematic illustration of the timeline of the study. IS, immune suppression. **(B)** Evaluation of mini-dystrophin expression by immunofluorescence staining using the flag-specific antibody (see Supplementary Fig. 2 for the enlarged image). Arrows indicate muscle tendon. **(C)** Evaluation of mini-dystrophin expression by Western blot using a dystrophin C-terminal domain specific antibody. Transgenic mdx, muscle lysate from ΔH2–R15 transgenic mdx mice. α-tubulin was used as the loading control. **(D)** Immunofluorescence staining with epitope-specific antibodies on serial sections from dual AAV treated ECU muscle. ΔH2–R15 mini-dystrophin carries the N-terminal domain, spectrin-like repeat 16 (R16), 17 (R17), hinge region 3 (H3), C-terminal domain, and a GFP gene fused in-frame to the C-terminus. However, it does not contain R4–6 and R11. Asterisks indicate the same myofiber in serial sections.

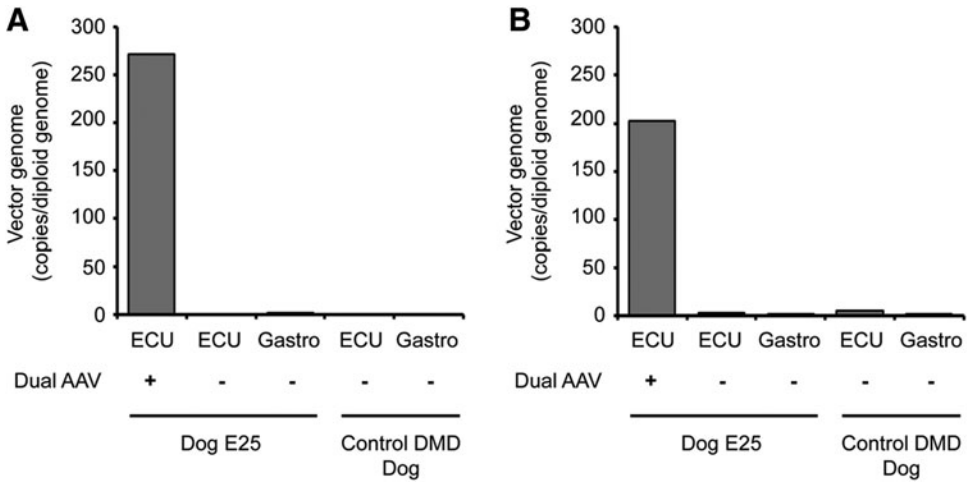

Figure 3. AAV genome copy quantification revealed accumulation of dual AAV vectors in the injected muscle. TaqMan quantitative PCR was performed to measure the AAV genome copy number in the treated and untreated ECU muscles and gastrocnemius muscle in Dog E25. Tissues from an affected dog that did not receive AAV injection were used as the negative control. **(A)** AAV genome copy number results for YL37. **(B)** AAV genome copy number results for YL39. ECU, extensor carpi ulnaris.

contralateral ECU muscle and the gastrocnemius muscle) and in the control un-injected dog (Fig. 3).

Dual AAV-mediated ΔH2–R15 mini-dystrophin expression restored the DGC complex, improved muscle histology and enhanced muscle function

A critical biochemical function of dystrophin is to assemble a series of transmembrane and cytosolic proteins into the DGC complex. On immunostaining, we observed restoration of these proteins (such as β-dystroglycan, β-sarcoglycan, dystrobrevin, and syntrophin) on the sarcolemma of mini-dystrophin positive myofibers (Fig. 4).

On HE staining, the dual AAV treated ECU muscle showed histology similar to that of the ECU muscle from a normal dog (Fig. 5A and B). In sharp contrast, the contralateral untreated ECU muscle displayed characteristic features of dystrophic pathology such as inflammation, degeneration/regeneration, and fibrosis (Fig. 5A and B). To further evaluate histological improvements, we quantified fibrosis, myofiber size distribution, and the percentage of muscle cells that contained centrally localized nuclei (Fig. 5C–E). On fibrosis quantification, we saw a $\sim$50% reduction in the treated ECU muscle compared to that of untreated ECU muscle (Fig. 5C). The myofiber size distribution was shifted towards that of the normal ECU muscle in the dual AAV treated ECU muscle but not in the buffer-injected contralateral ECU muscle. The peak myofiber size in the normal ECU muscle was 26^2 to 28^2 μm^2 (675 to 785 μm^2). The peak myofiber size in the affected dog ECU muscle was $\sim 38^2$ μm^2 ($\sim$1,440 μm^2). On the untreated ECU muscle in dog E25, the peak myofiber size was 44^2 μm^2 ($\sim$1,940 μm^2). On the treated side, the peak myofiber size showed a substantial shift toward normalization to 31^2 μm^2 ($\sim$960 μm^2) (Fig. 5D). The presence of centrally nucleated myofibers is a cellular marker for muscle degeneration/regeneration. We detected a 50% reduction in dual AAV treated muscle, suggesting an amelioration of muscle degeneration and regeneration (Fig. 5E).

Improvement of muscle strength is the ultimate goal of DMD therapy. To this end, we measured ECU muscle function using a previously published *in situ* force assay protocol (Fig. 6; Table 1).[31,35] Compared with that of untreated dystrophic ECU muscles, the specific twitch tension and specific isometric tension were substantially increased following mini-dystrophin treatment (Fig. 6A). Eccentric contraction is a highly damaging form of muscle contraction in which a contracting muscle is lengthened by external force. The ability to preserve muscle force following eccentric contraction has been considered a gold standard in evaluating muscle function in the field of muscular dystrophy gene therapy. Remarkably, the force of the dual AAV treated ECU muscle was better preserved than that of untreated ECU muscles through ten rounds of eccentric contraction (Fig. 6B).

DISCUSSION

In this study, we show proof-of-principle evidence that dual AAV-delivery of a large therapeutic *dystrophin* gene can effectively reconstitute

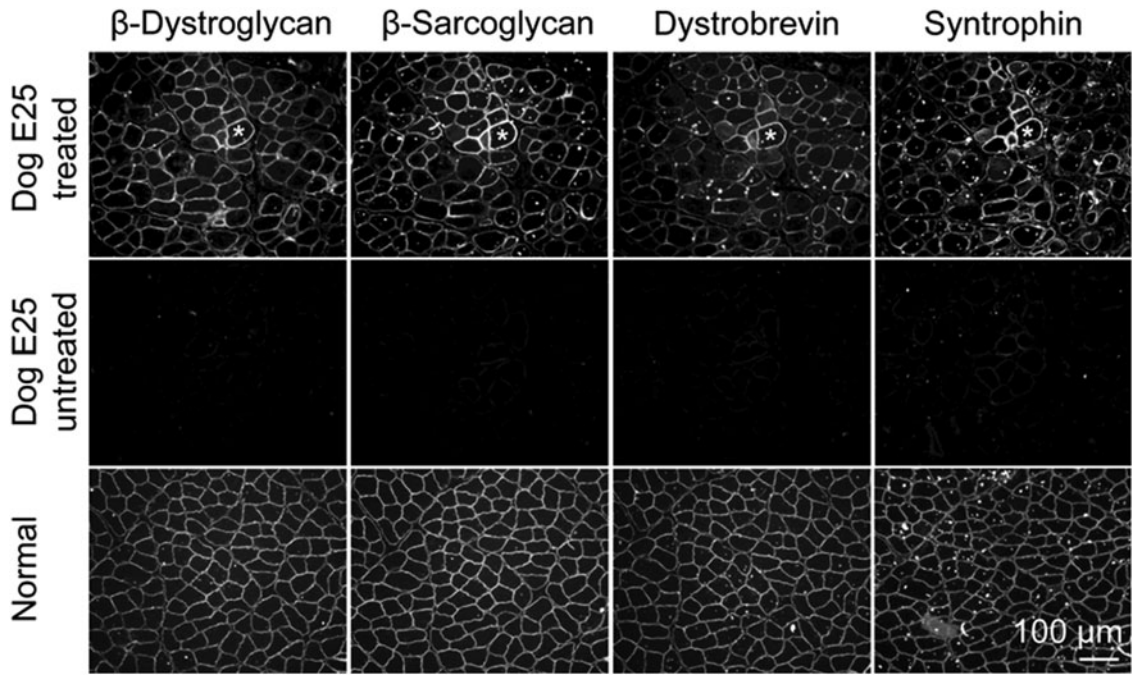

Figure 4. Dual AAV mini-dystrophin expression restored of major components of the DGC. Immunofluorescence staining for β-dystroglycan, β-sarcoglycan, dystrobrevin and syntrophin. Muscle in the top panels comes from the same serial sections shown in Figure 2D. Asterisk, the same myofiber in serial sections. DGC, dystrophin-associated glycoprotein complex.

dystrophin expression in diseased muscle in the canine DMD model. Importantly, dual AAV therapy resulted in biochemical, histological, and physiological improvements.

The development of the dual AAV technology has been recognized as a major breakthrough in the history of AAV gene therapy.[54,55] AAV vectors have many features that are highly desirable for gene therapy, such as the superior safety of the wild-type virus, gut-less nature of the vector, long-term persistence as an episomal molecule, easy production and purification, and versatile tissue tropism through capsid modification. However, AAV is among the smallest existing viruses. The maximal genome size that can be packaged in a fully assembled AAV particle is merely 5 kb. This creates a challenge in using AAV to deliver therapeutic expression cassettes that are larger than 5 kb. Dual AAV vector technology offers a solution to this problem. In dual AAV vectors, a large therapeutic gene is expressed through intermolecular recombination of the vector genomes. Application of this technology in mouse models of human diseases has revealed marvelous therapeutic promise in treating blood, retinal, and muscle diseases.[11,12,17,22–25,56]

The ultimate goal of gene therapy is to treat diseased large mammals, including human patients and/or veterinary patients (such as dogs and cats). Although others have shown efficient dual AAV-mediated gene transfer in normal pigs and nonhuman primates,[57,58] dual AAV technology has never been evaluated in a diseased model in large mammals. Failure to translate mouse results to human patients has been a major bottleneck in the development of experimental therapies for DMD and many other diseases.[59–61] This is at least partially because mouse models (such as the commonly used mdx model for DMD) are built on inbred mice and they show minimal clinical disease.[62] Further the small size of the mouse makes it impossible to test the scale-up. Studies performed in large animal models will help bridge the translational gap between mice and patients.[63,64]

Against this backdrop, we explored dual AAV gene therapy in the canine DMD model.[62] To our knowledge, this is the first study to evaluate dual AAV vectors in a diseased large mammal. As a starting point, we performed local therapy in a single muscle (ECU) in a severely affected adult dog. The contralateral ECU muscle was used as the untreated control. AAV genome quantification confirmed the delivery of the dual AAV vectors in the treated ECU muscle (Fig. 3). We have previously used the same local injection approach to study single AAV *micro-dystrophin* (ΔR2–15/ΔR18–19/

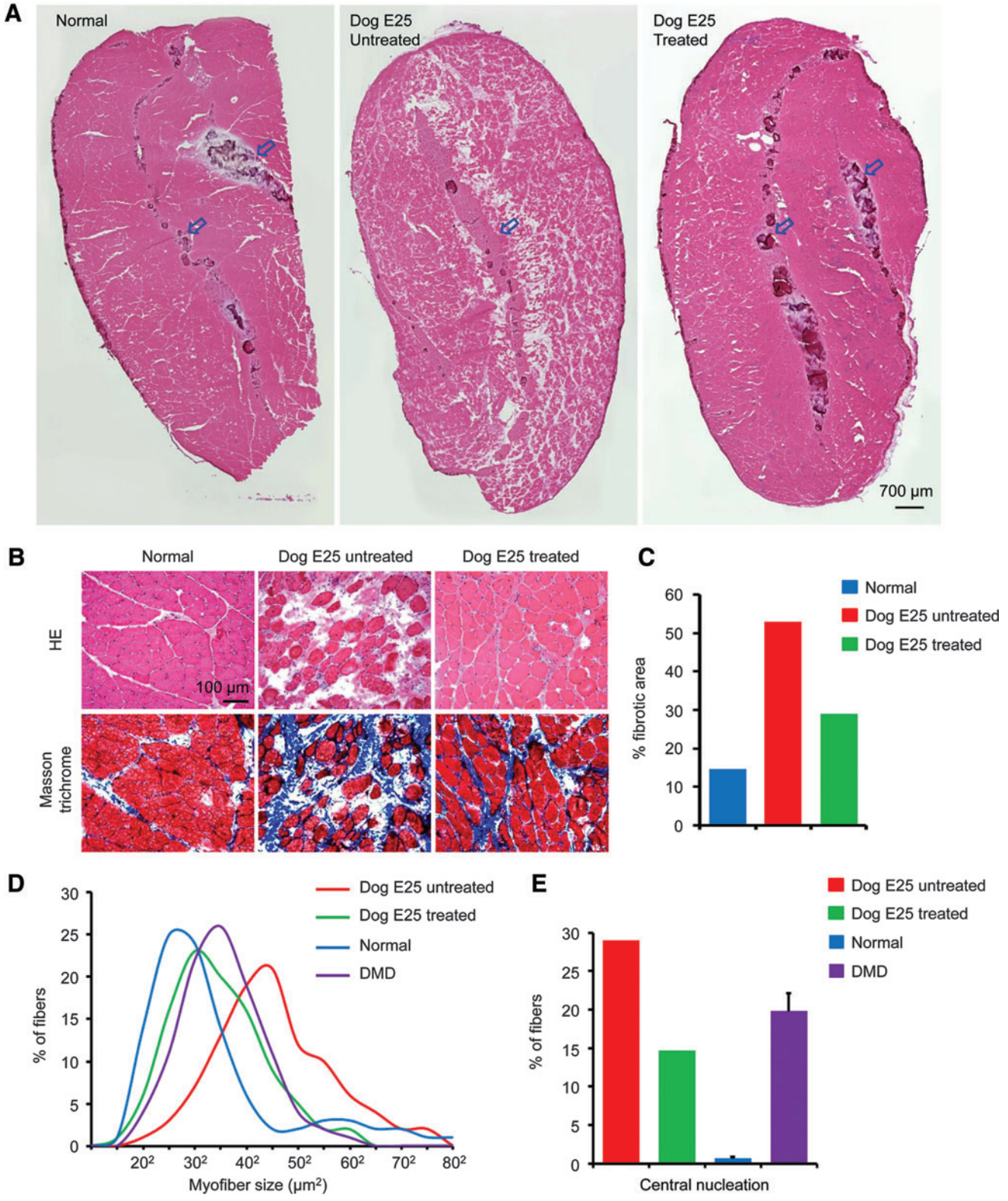

Figure 5. Dual AAV ΔH2–R15 mini-dystrophin treatment ameliorated dystrophic histopathology in dog muscle. **(A)** Representative low magnification view of hematoxylin and eosin stained sections from the normal ECU muscle (*left panel*), dog E25's buffer-injected ECU muscle (*middle panel*) and dog E25's dual AAV-injected ECU muscle (*right panel*). *Arrows* indicate muscle tendon. **(B)** Representative high magnification view of hematoxylin and eosin (*top panels*) and Masson trichrome (*bottom*) stained ECU muscle sections from the indicated dogs. On Masson trichrome staining, fibrotic tissue is in blue color. **(C)** Morphometric quantification of fibrosis. **(D)** Myofiber size distribution in the ECU muscle of normal dogs (n=9,661 myofibers from 6 dogs), control DMD dogs (n=5,055 myofibers from 4 dogs), and dog E25 (untreated side, n=607 myofibers; dual AAV treated side, n=560 myofibers). **(E)** Quantification of central nucleation. Central nucleation shows the percentage of the myofibers with centrally localized nuclei. It is a biomarker for muscle degeneration and regeneration. Normal, 10,449 myofibers from the ECU muscle of six normal dogs; DMD, 7,482 myofibers from eight control DMD dogs; Dog E25 untreated, 602 myofibers from the ECU muscle on the buffer injected side; Dog E25 treated, 488 myofibers from the ECU muscle on the dual AAV-injected side. Color images available online at www.liebertpub.com/hum

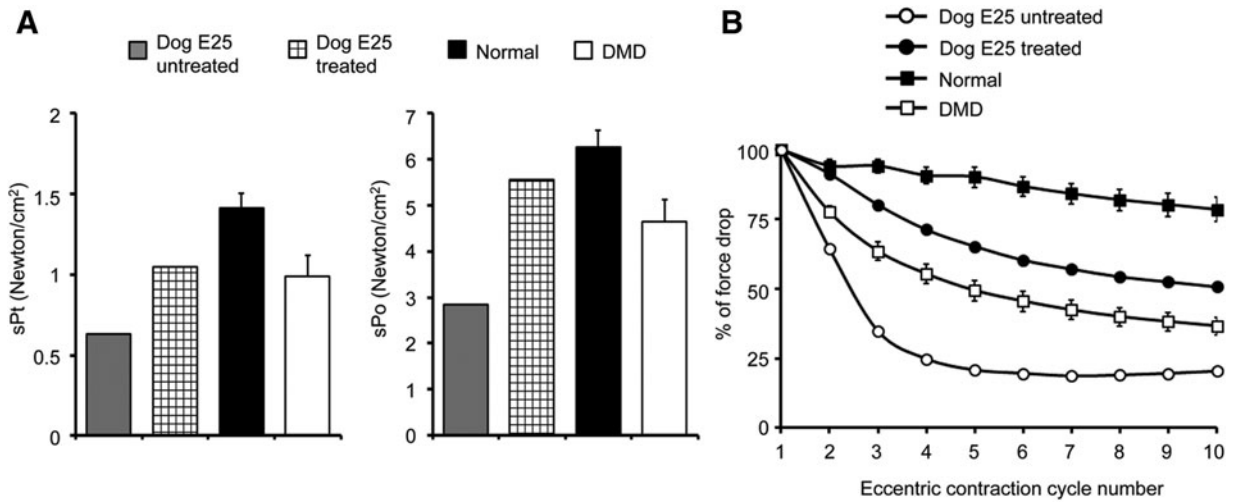

Figure 6. Dual AAV ΔH2-R15 mini-dystrophin therapy improved muscle contractility. **(A)** *Left panel* shows the specific twitch force (sPt). *Right panel* shows the specific tetanic force (sPo). **(B)** Relative changes of the tetanic force over 10 cycles of eccentric contraction in the normal, control DMD, dog E25's buffer-injected (untreated), and dog E25's dual AAV-injected (treated) ECU muscles. For both **A** and **B**, $n=12$ for control DMD dogs and $n=11$ for normal dogs.

ΔR20–23/ΔC) gene therapy in dystrophic dogs.[31] Similar to what we have observed in the single AAV micro-dystrophin study,[31] we obtained widespread mini-dystrophin expression in more than 50% of the myofibers on muscle cross-section by immunostaining (Fig. 2B; Supplementary Fig. S2). On western blot, the total amount of the dystrophin protein produced from the single microgene AAV vector reached the similar level or even above that of a normal dog.[31] Interestingly, the total amount of the dystrophin protein produced from the minigene dual AAV vectors seemed much lower than that of a normal dog (Fig. 2C)[31] There are several possible explanations for similar expression on immunostaining (in terms of the percentage of dystrophin positive cells) but lower expression on Western blot (in terms of the absolute dystrophin quantity in muscle). Skeletal muscle cells are multinucleated. RNA transcripts from a single transduced myonucleus can spread through a broad region for protein translation. On immunostaining, the myofiber will present as dystrophin positive. Western blot is a different measure; it quantifies the total amount of protein generated in the muscle cell. In the case of the single AAV approach, every vector genome in the myonuclei is transcriptionally competent. In the case of dual AAV approach, only a fraction of the vector genome can recombine into the transcriptionally competent expression cassette. Hence, the absolute amount of the protein being generated from dual AAV vectors will be less.

Next, we examined whether dual AAV minigene therapy could benefit the dystrophic muscle. On immunostaining, mini-dystrophin expression effectively restored components of the DGC to the sarcolemma (Fig. 4). On HE staining and Masson trichrome staining, the treated ECU muscle was clearly improved (Fig. 5). To gain a better understanding on the level of improvement, we performed several quantitative assays. Quantification of fibrosis revealed a clear reduction in the muscle that had received the dual AAV minigene vectors (Fig. 5C). When we compared the myofiber size distribution curve of the untreated ECU muscle in the dog E25 (the one used for dual AAV injection) to that of the ECU muscle of the control DMD dogs, interestingly, we found a rightward shift of the curve (Fig. 5D). Further the curve was broadened in dog E25's untreated ECU muscle (Fig. 5D). This suggests that dog E25 had more severe muscle disease than the control DMD dogs. Further analysis confirmed that this was indeed the case. For example, the untreated

Table 1. *Age, body weight and anatomical properties of the extensor carpi ulnaris muscle*

	Duan Lab Colony		*Dog E25 (DMD)*	
	Normal (n = 11)	*DMD (n = 12)*	*Treated*	*Untreated*
Age (months)	14.53 ± 5.77	8.78 ± 3.76	14.2	
Body weight (kg)	15.26 ± 1.54	9.40 ± 2.18	18	
ECU muscle				
Weight (g)	5.07 ± 1.00	3.52 ± 0.54	6.53	7.13
Weight (g/kg body weight)	0.33 ± 0.07	0.39 ± 0.08	0.36	0.40
Length (cm)	11.95 ± 1.54	10.64 ± 1.47	13.86	13.86
PCSA (cm^2)	10.46 ± 1.21	6.93 ± 1.03	11.67	12.75

DMD, Duchenne muscular dystrophy; ECU, extensor carpi ulnaris; PCSA, physiological cross-sectional area.

ECU muscle of dog E25 had more centrally nucleated myofibers than the ECU muscle of the control DMD dogs (Fig. 5E). On physiological evaluation of the specific twitch force, specific tetanic force, and the eccentric contraction profile, dog E25's treated ECU muscle outperformed that of the untreated ECU muscle (Fig. 6). Collectively, our results suggest that dual AAV mediated expression of mini-dystrophin can ameliorate biochemical, histological, and physiological defects in the canine DMD model.

During our quantitative analysis, we found that the experimental dog (dog E25) appeared to have a much more severe dystrophic phenotype than the negative population control of untreated DMD dogs. Two factors may account for this observation. First, dog E25 (age 14.2 months) was older than the control DMD dogs (age 8.78 ± 3.76 months) (Table 1). DMD is a progressive muscle disease. Patients get worse as they get older. Second, dog E25 (body weight, 18 kg) was larger than control DMD dogs (body weight 9.40 ± 2.18 kg) used in this study (Table 1). Mathematical modeling suggests that larger subjects are more affected.[65] Indeed, it has been shown that larger affected dogs have more severe disease.[66]

AAV-mediated *micro-dystrophin* gene therapy is currently on the forefront of *dystrophin* gene replacement therapy for DMD. Several groups have publicly announced plans for clinical trials in the near future. On the other hand, AAV mini-dystrophin therapy has lagged behind. Although we only have a limited sample size ($n = 1$ ECU muscle in one dog), we reasoned that a comparison with our previously published microgene therapy results ($n = 8$ ECU muscles in six dogs) would provide some perspective for future development of DMD gene replacement.[31] In the current dual AAV minigene study, we treated a dog that appeared to have a more severe phenotype and also we detected less dystrophin expression on western blot (Fig. 2; Table 1). With this in mind, we initially thought that dual AAV therapy in dog E25 would yield less protection than what we have seen with AAV micro-dystrophin therapy.[31] Surprisingly, both qualitative and quantitative assays suggest that this was not the case. For example, central nucleation was not improved by micro-dystrophin therapy.[31] However, mini-dystrophin treatment resulted in $\sim 50\%$ improvement in centronucleation (Fig. 5E). Specific muscle force was barely increased following micro-dystrophin therapy but it was doubled following mini-dystrophin therapy (Fig. 6A).[31] The most striking is the improvement in the eccentric contraction profile (Fig. 6B). After one round of eccentric contraction, the force drop was completely prevented with dual AAV mini-dystrophin therapy but only partially prevented with single AAV micro-dystrophin therapy (Fig. 6B).[31] After five rounds of eccentric contraction, dual AAV mini-dystrophin therapy was still able to protect the muscle from damage-induced force drop, but protection was completely lost with single AAV micro-dystrophin therapy (Fig. 6B).[31] While these observations remain preliminary and require confirmation with comprehensive studies in the future, we speculate that there may indeed exist a biological foundation for the seemingly superior performance with dual AAV minigene therapy. First, patient studies have shown that a larger dystrophin protein is associated with a milder clinical disease.[6] Second, transgenic studies have demonstrated consistently that mini-dystrophin yields better rescue than micro-dystrophin.[8] Third, we believe that the addition of more functional domains in mini-dystrophin may have played an important role. These domains include the R1–3 membrane binding domain, R16–19 putative cardiac domain, R20–23 microtubule binding domain, and syntrophin and dystrobrevin binding domain (Duan lab, unpublished data).[13,31,44,45,48,51,67]

While our data are highly encouraging, there are important limitations. First, we have only treated one dog. Additional studies with a large sample size are absolutely needed to corroborate the findings of the current study. Second, we only treated the dog for 2 months (we did this intentionally so that the data can be compared with the micro-dystrophin data we published before).[31] Long-term study is needed to determine whether dual AAV can provide persistent protection. Ideally, micro-dystrophin therapy should be included in the long-term study for a side-by-side comparison to see if mini-dystrophin can still outperform micro-dystrophin. Third, as a proof-of-concept study, we have opted to do local injection. While local therapy can benefit patients and improve their life quality,[68] systemic delivery would be preferred for body-wide correction.[69] Systemic dual AAV mini-dystrophin therapy should be explored in the future. Fourth, we only tested dual AAV in dystrophic dog limb muscle. Considering the prevalence of respiratory and cardiac complications in DMD/Becker muscular dystrophy patients, it will be important to evaluate therapeutic benefit of dual AAV therapy in the diaphragm as well as the heart, especially in light of the putative heart protection domain in mini-dystrophin (Duan lab, unpublished data). Lastly, little is known about the molecular fate of the reconstituted vector genome following long-term dual AAV therapy. This should be included in future studies.

ACKNOWLEDGMENTS

This study was supported by grants from Hope for Javier, Jackson Freel DMD Research Fund, and National Institutes of Health (AR-67985). The funders had no role in study design, data collection and analysis, decision to publish, or preparation of the manuscript. We thank Dr. Arun Srivastava (University of Florida, Gainesville, FL) for providing Y731F AAV-9 packaging plasmid, Dr. Jeffrey Chamberlain (University of Washington, Seattle, WA) for providing the dystrophin N-terminal domain specific polyclonal antibody, and Dr. Glenn Morris (Robert Jones and Agnes Hunt Orthopaedic Hospital) for providing epitope-specific dystrophin monoclonal antibodies. We thank Brittney Haffner and Tony Cheng for technical help with AAV genome copy number quantification.

AUTHOR DISCLOSURE

D.D. is a member of the scientific advisory board for Solid Biosciences and an equity holder of Solid Biosciences, as well as an inventor on a patent licensed to Solid Biosciences C. The Duan lab has received research support from Solid Biosciences.

REFERENCES

1. Kunkel LM. 2004 William Allan award address. cloning of the DMD gene. Am J Hum Genet 2005;76:205–214.
2. Koenig M, Hoffman EP, Bertelson CJ, et al. Complete cloning of the Duchenne muscular dystrophy (DMD) cDNA and preliminary genomic organization of the DMD gene in normal and affected individuals. Cell 1987;50:509–517.
3. Lai Y, Yue Y, Duan D. Evidence for the failure of adeno-associated virus serotype 5 to package a viral genome > or = 8.2 kb. Mol Ther 2010;18:75–79.
4. Dong JY, Fan PD, Frizzell RA. Quantitative analysis of the packaging capacity of recombinant adeno-associated virus. Hum Gene Ther 1996;7:2101–2112.
5. Dong B, Nakai H, Xiao W. Characterization of genome integrity for oversized recombinant AAV vector. Mol Ther 2010;18:87–92.
6. Fanin M, Freda MP, Vitiello L, et al. Duchenne phenotype with in-frame deletion removing major portion of dystrophin rod: threshold effect for deletion size? Muscle Nerve 1996;19:1154–1160.
7. England SB, Nicholson LV, Johnson MA et, al. Very mild muscular dystrophy associated with the deletion of 46% of dystrophin. Nature 1990;343: 180–182.
8. Harper SQ, Hauser MA, DelloRusso C, et al. Modular flexibility of dystrophin: implications for gene therapy of Duchenne muscular dystrophy. Nat Med 2002;8:253–261.
9. Lai Y, Thomas GD, Yue Y, et al. Dystrophins carrying spectrin-like repeats 16 and 17 anchor nNOS to the sarcolemma and enhance exercise performance in a mouse model of muscular dystrophy. J Clin Invest 2009;119:624–635.
10. Lai Y, Zhao J, Yue Y, et al. Alpha2 and alpha3 helices of dystrophin R16 and R17 frame a microdomain in the alpha1 helix of dystrophin R17 for neuronal NOS binding. Proc Natl Acad Sci U S A 2013;110:525–530.
11. Zhang Y, Duan D. Novel *mini-dystrophin* gene dual adeno-associated virus vectors restore neuronal nitric oxide synthase expression at the sarcolemma. Hum Gene Ther 2012;23:98–103.
12. Zhang Y, Yue Y, Li L, et al. Dual AAV therapy ameliorates exercise-induced muscle injury and functional ischemia in murine models of Duchenne muscular dystrophy. Hum Mol Genet 2013;22:3720–3729.
13. Zhao J, Kodippili K, Yue Y, et al. Dystrophin contains multiple independent membrane-binding domains. Hum Mol Genet 2016;25:3647–3653.
14. Duan D, Yue Y, Yan Z, et al. A new dual-vector approach to enhance recombinant adeno-associated virus-mediated gene expression through intermolecular cis activation. Nat Med 2000;6:595–598.
15. Yan Z, Zhang Y, Duan D, et al. Trans-splicing vectors expand the utility of adeno-associated virus for gene therapy. Proc Natl Acad Sci U S A 2000;97:6716–6721.
16. Duan D, Yue Y, Engelhardt JF. Expanding AAV packaging capacity with trans-splicing or overlapping vectors: a quantitative comparison. Mol Ther 2001;4:383–391.
17. Ghosh A, Yue Y, Lai Y, et al. A hybrid vector system expands aden-associated viral vector packaging capacity in a transgene independent manner. Mol Ther 2008;16:124–130.
18. Ghosh A, Yue Y, Duan D. Efficient transgene reconstitution with hybrid dual AAV vectors carrying the minimized bridging sequence. Hum Gene Ther 2011;22:77–83.
19. Ghosh A, Duan D. Expending adeno-associated viral vector capacity: a tale of two vectors. Biotechnol Genet Eng Rev 2007;24:165–177.
20. Chamberlain K, Riyad JM, Weber T. Expressing transgenes that exceed the packaging capacity of adeno-associated virus capsids. Hum Gene Ther Methods 2016;27:1–12.
21. Hirsch ML, Wolf SJ, Samulski RJ. Delivering transgenic DNA exceeding the carrying capacity of AAV vectors. Methods Mol Biol 2016;1382: 21–39.
22. Lai Y, Yue Y, Liu M, et al. Efficient in vivo gene expression by trans-splicing adeno-associated viral vectors. Nat Biotechnol 2005;23:1435–1439.
23. Ghosh A, Yue Y, Shin J-H, et al. Systemic trans-splicing AAV delivery efficiently transduces the heart of adult mdx mouse, a model for Duchenne muscular dystrophy. Hum Gene Ther 2009;20:1319–1328.
24. Ghosh A, Yue Y, Long C, et al. Efficient whole-body transduction with trans-splicing adeno-associated viral vectors. Mol Ther 2007;15:750–755.
25. Odom GL, Gregorevic P, Allen JM, et al. Gene therapy of mdx mice with large truncated dystrophins generated by recombination using rAAV6. Mol Ther 2011;19:36–45.
26. Smith BF, Yue Y, Woods PR, et al. An intronic LINE-1 element insertion in the *dystrophin* gene aborts dystrophin expression and results in Duchenne-like muscular dystrophy in the Corgi breed. Lab Invest 2011;91:216–231.
27. Fine DM, Shin JH, Yue Y, et al. Age-matched comparison reveals early electrocardiography and echocardiography changes in dystrophin-deficient dogs. Neuromuscul Disord 2011;21:453–461.
28. Sharp NJ, Kornegay JN, Van Camp SD, et al. An error in dystrophin mRNA processing in golden retriever muscular dystrophy, an animal homologue of Duchenne muscular dystrophy. Genomics 1992;13:115–121.
29. Petrs-Silva H, Dinculescu A, Li Q, et al. High-efficiency transduction of the mouse retina by tyrosine-mutant AAV serotype vectors. Mol Ther 2009;17:463–471.
30. Shin JH, Yue Y, Duan D. Recombinant adeno-associated viral vector production and purification. Methods Mol Biol 2012;798:267–284.
31. Shin JH, Pan X, Hakim CH, et al. Microdystrophin ameliorates muscular dystrophy in the canine model of Duchenne muscular dystrophy. Mol Ther 2013;21:750–757.
32. Hakim CH, Yue Y, Shin JH, et al. Systemic gene transfer reveals distinctive muscle transduction

profile of tyrosine mutant AAV-1, -6, and -9 in neonatal dogs. Mol Ther Methods Clin Dev 2014;1: 14002.

33. Yue Y, Pan X, Hakim CH, et al. Safe and bodywide muscle transduction in young adult Duchenne muscular dystrophy dogs with adeno-associated virus. Hum Mol Genet 2015;24:5880–5890.
34. Shin JH, Yue Y, Srivastava A, et al. A simplified immune suppression scheme leads to persistent micro-dystrophin expression in Duchenne muscular dystrophy dogs. Hum Gene Ther 2012;23:202–209.
35. Yang HT, Shin JH, Hakim CH, et al. Dystrophin deficiency compromises force production of the extensor carpi ulnaris muscle in the canine model of Duchenne muscular dystrophy. PLoS One 2012; 7:e44438.
36. Kodippili K, Vince L, Shin JH, et al. Characterization of 65 epitope-specific dystrophin monoclonal antibodies in canine and murine models of Duchenne muscular dystrophy by immunostaining and western blot. PLoS One 2014;9:e88280.
37. Wasala NB, Lai Y, Shin JH, et al. Genomic removal of a therapeutic *mini-dystrophin* gene from adult mice elicits a Duchenne muscular dystrophy-like phenotype. Hum Mol Genet 2016;25:2633–2644.
38. Bhosle RC, Michele DE, Campbell KP, et al. Interactions of intermediate filament protein synemin with dystrophin and utrophin. Biochem Biophys Res Commun 2006;346:768–777.
39. Reynolds JG, McCalmon SA, Donaghey JA, et al. Deregulated protein kinase A signaling and myospryn expression in muscular dystrophy. J Biol Chem 2008;283:8070–8074.
40. Ayalon G, Davis JQ, Scotland PB, et al. An ankyrin-based mechanism for functional organization of dystrophin and dystroglycan. Cell 2008;135: 1189–1200.
41. Rezniczek GA, Konieczny P, Nikolic B, et al. Plectin 1f scaffolding at the sarcolemma of dystrophic (mdx) muscle fibers through multiple interactions with beta-dystroglycan. J Cell Biol 2007; 176:965–977.
42. Ishikawa-Sakurai M, Yoshida M, Imamura M, et al. ZZ domain is essentially required for the physiological binding of dystrophin and utrophin to beta-dystroglycan. Hum Mol Genet 2004;13:693–702.
43. Huang X, Poy F, Zhang R, et al. Structure of a WW domain containing fragment of dystrophin in complex with beta-dystroglycan. Nat Struct Biol 2000;7:634–638.
44. Newey SE, Benson MA, Ponting CP, et al. Alternative splicing of dystrobrevin regulates the stoichiometry of syntrophin binding to the dystrophin protein complex. Curr Biol 2000;10:1295–1298.
45. Sadoulet-Puccio HM, Rajala M, Kunkel LM. Dystrobrevin and dystrophin: an interaction through coiled-coil motifs. Proc Natl Acad Sci U S A 1997; 94:12413–12418.
46. Ursitti JA, Lee PC, Resneck WG, et al. Cloning and characterization of cytokeratins 8 and 19 in adult rat striated muscle. Interaction with the dystrophin glycoprotein complex. J Biol Chem 2004;279: 41830–41838.
47. Prins KW, Humston JL, Mehta A, et al. Dystrophin is a microtubule-associated protein. J Cell Biol 2009;186:363–369.
48. Belanto JJ, Mader TL, Eckhoff MD, et al. Microtubule binding distinguishes dystrophin from utrophin. Proc Natl Acad Sci U S A 2014;111:5723–5728.
49. Banuelos S, Saraste M, Djinovic Carugo K. Structural comparisons of calponin homology domains: implications for actin binding. Structure 1998;6:1419–1431.
50. Norwood FL, Sutherland-Smith AJ, Keep NH, et al. The structure of the N-terminal actin-binding domain of human dystrophin and how mutations in this domain may cause Duchenne or Becker muscular dystrophy. Structure 2000;8:481–491.
51. Nigro G, Politano L, Nigro V, et al. Mutation of *dystrophin* gene and cardiomyopathy. Neuromuscul Disord 1994;4:371–379.
52. Lostal W, Kodippili K, Yue Y, et al. Full-length dystrophin reconstitution with adeno-associated viral vectors. Hum Gene Ther 2014;25:552–562.
53. Wang Z, Kuhr CS, Allen JM, et al. Sustained AAV-mediated dystrophin expression in a canine model of Duchenne muscular dystrophy with a brief course of immunosuppression. Mol Ther 2007;15:1160–1166.
54. Flotte TR. Size does matter: overcoming the adeno-associated virus packaging limit. Respir Res 2000;1: 16–18.
55. Samulski RJ. Expanding the AAV package. Nat Biotechnol 2000;18:497–498.
56. Lostal W, Bartoli M, Bourg N, et al. Efficient recovery of dysferlin deficiency by dual adeno-associated vector-mediated gene transfer. Hum Mol Genet 2010;19:1897–1907.
57. Colella P, Trapani I, Cesi G, et al. Efficient gene delivery to the cone-enriched pig retina by dual AAV vectors. Gene Ther 2014;21:450–456.
58. Sondergaard PC, Griffin DA, Pozsgai ER, et al. AAV.Dysferlin overlap vectors restore function in dysferlinopathy animal models. Ann Clin Transl Neurol 2015;2:256–270.
59. Mendell JR, Kissel JT, Amato AA, et al. Myoblast transfer in the treatment of Duchenne's muscular dystrophy. N Engl J Med 1995;333:832–838.
60. Wagner KR, Fleckenstein JL, Amato AA, et al. A phase I/IItrial of MYO-029 in adult subjects with muscular dystrophy. Ann Neurol 2008;63: 561–571.
61. Birmingham K. Controversial muscular dystrophy therapy goes to court. Nat Med 1997;3: 1058.
62. McGreevy JW, Hakim CH, McIntosh MA, et al. Animal models of Duchenne muscular dystrophy: from basic mechanisms to gene therapy. Dis Model Mech 2015;8:195–213.
63. Duan D. Duchenne muscular dystrophy gene therapy: lost in translation? Res Rep Biol 2011;2: 31–42.
64. Duan D. Duchenne muscular dystrophy gene therapy in the canine model. Hum Gene Ther Clin Dev 2015;26:57–69.
65. Bodor M, McDonald CM. Why short stature is beneficial in Duchenne muscular dystrophy. Muscle Nerve 2013;48:336–342.
66. Valentine BA, Cooper BJ, de Lahunta A, et al. Canine X-linked muscular dystrophy–an animal model of Duchenne muscular dystrophy: clinical studies. J Neurol Sci 1988;88:69–81.
67. Koo T, Malerba A, Athanasopoulos T, et al. Delivery of AAV2/9-microdystrophin genes incorporating helix 1 of the coiled-coil motif in the C-terminal domain of dystrophin improves muscle pathology and restores the level of alpha1-syntrophin and alpha-dystrobrevin in skeletal muscles of mdx mice. Hum Gene Ther 2011;22:1379–1388.
68. Mendell JR, Sahenk Z, Malik V, et al. A phase I/IIa follistatin gene therapy trial for Becker muscular dystrophy. Mol Ther 2015;23:192–201.
69. Duan D. Systemic delivery of adeno-associated viral vectors. Curr Opin Virol 2016;21:16–25.

Received for publication May 19, 2017;
accepted after revision August 3, 2017.

Published online: August 4, 2017.